Annals of Biomedical Engineering, Vol. 43, No. 7, July 2015 *(© 2014)* pp. 1571–1584
DOI: 10.1007/s10439-014-1219-x

Analysis of Low Density Lipoprotein (LDL) Transport Within a Curved Artery

SHUJUAN WANG and KAMBIZ VAFAI

Department of Mechanical Engineering, University of California, Riverside, CA 92521, USA

(Received 30 September 2014; accepted 8 December 2014; published online 20 December 2014)

Associate Editor Gerhard A. Holzapfel oversaw the review of this article.

Abstract—To elucidate the mechanism of the effect of LDL concentration on the thickening of intima in a curved artery, LDL transport in each layer of the curved arterial wall is studied analytically. A comprehensive concentration distribution expression of LDL in each layer of the curved artery wall is presented along with the characterization and estimation of the effect of curvature on the growth of atherosclerosis within the arterial wall. The effect of curvature on species concentration distribution is analyzed and the results are thoroughly benchmarked against prior pertinent works. The concentration at the interface of lumen and endothelium will directly affect the concentration profile inside the arterial wall layers. The results show that the average concentration in the circumferential direction is actually decreasing in the axial direction for a curved artery compared with a straight artery. Small radius ratio and Reynolds number will augment the LDL accumulation at the lumen endothelium interface. The increase in concentration at the lumen/endothelium interface in the axial direction has a minor effect on the concentration profile at the other wall interface layers.

Keywords—Low-density lipoprotein transport, Curvature, Arterial wall, Atherosclerosis.

NOMENCLATURE

c	LDL concentration
Dn	Dean number $\mathrm{Dn} = 2\sqrt{\lambda}\mathrm{Re}$
Re	Reynolds number $\mathrm{Re} = \rho v 2 r_0/\mu$
D	LDL diffusivity
De	Effective LDL diffusivity
F	Dimensionless inertia coefficient
λ	Ratio of artery radius to curvature radius r_0/R
$\mathbf{V}$	Velocity vector
p	Hydraulic pressure
ρ	Fluid density
δ	Porosity
μ	Dynamic viscosity
L	Length of the artery
R	Radius of the curvature
σ	Reflection coefficient
y	$y = r_0 - r$
r_0	Radius of the lumen domain
k	Reaction coefficient
r	Radial coordinate
K	Permeability
E	De/r_0^2
Δ	Thickness of concentration boundary layer

Symbol

$\langle\rangle$	Local volume average

Subscripts and Superscripts

F	Fluid
I	$i = 0$, 1, 2, 3 and 4 representing lumen, endothelium, intima, IEL, and media, respectively
70 mmHg	Refers to properties with a gauge pressure of 70 mmHg
eff, e	Refers to an effective property
end	Refers to the endothelium layer
w	Wall
$+$	Non-dimensional parameter

INTRODUCTION

The American Heart Association[21] reports that the number of American adults with cardiovascular

Address correspondence to Kambiz Vafai, Department of Mechanical Engineering, University of California, Riverside, CA 92521, USA. Electronic mail: vafai@engr.ucr.edu

diseases (CVD) is close to 80 million which means that one out of 2.8 persons dies due to a cardiovascular disease. A major contributor of CVD, atherosclerosis is caused by the abnormal accumulation of macromolecules, such as lipoprotein, within the arterial wall. The accumulation of macromolecules leads to the narrowing and occlusion of the artery. The mechanism of atherogenic low-density lipoproteins transport from lumen to arterial wall and the concentration polarization needs to be elucidated.

In vivo observation also shows the localization of atherosclerotic lesions in the artery, mainly at certain sites such as the walls of the curved artery. As discussed later, a number of studies[25] have shown that some CVD including atherosclerosis are prone to occur in curved arteries, such as coronary arteries, as curvature will cause abnormal changes of blood flow. This phenomenon has attracted much attention of the researchers in figuring out the relationship between the flow and preferred location of atherosclerosis.[25] The curvature may lead to the occurrence of secondary flow and vortex, which causes alteration of shear distribution along an arterial wall. Several research works[25] have hypothesized that the local hemodynamics plays an important role in pathogenesis, such as the formation and development of atherosclerosis. The changes in blood flow will apparently impact the thickening of the endothelium and the proliferation of the smooth muscle cells, which may lead to CVD such as atherosclerosis and thrombosis. Thus the irregular shape and geometry of the arteries may aggravate the formation and development of atherosclerosis. As such, it is very important to study the hemodynamic mechanism in curved arteries to find out how local flow characteristics may affect the formation of atherosclerosis.

The role of a hemodynamic mechanism on the concentration polarization of an arterial wall is still not fully understood. Several studies have been performed on the effect of the wall shear stress at the interface of lumen and endothelium. Chang and Tarbell[7] numerically studied the complex secondary flows with up to seven vortices in the half tube. Their study reveals that peak axial wall shear stress appears on the outside wall in steady flow and lowest mean wall shear stress on the inside wall, however, the highest instantaneous wall shear stress and r.m.s wall shear stress also appears on the inside wall. The influence of the likely shear stress (mean wall shear stress or r.m.s shear stress) changes with the timescale.

Dennis and Ng[12] numerically studied the steady laminar flow through a slightly curved tube and presented two solutions to Navier–Stokes equation in different Dean number regions respectively. Qiao *et al.*[20]and Wada and Karino[25] also numerically studied the flow in a curved artery with multiple bends to find out the effect of flow in the lumen on the shear stress and LDL concentration distribution at lumen and endothelium surface. Dash *et al.*[11] and Padmanabhan[19] presented an analytical model for the effect of the curvature on the pressure drop, impedance and wall shear stress based on a perturbation analysis. Yasuo and Watara[30] also carried out a theoretical study of the developed laminar flow in a curved pipe. In their work, the flow in the pipe is divided into a core region and a boundary layer at large Dean numbers based on whether the viscous stress can be ignored. The velocity distribution in the boundary layer was derived in their work. It should be noted that the concentration distribution within a curved artery wall was not considered in these works.

In many research works, wall shear stress is considered to be the major cause of localization resulting atherosclerosis. The wall shear stress affects LDL accumulation and atherosclerosis mainly occurs at regions of low wall shear stress. However, *in vivo* experiments shows regions of high LDL do not always correspond to the lowest wall shear stress area. It should be noted that the LDL concentration in the wall is mainly determined by the flow pattern within the wall. In order to elucidate the mechanisms of atherogenesis, the investigation of LDL behavior in the arterial wall layers must be better understood. Thus the mechanism of the mass transfer in each layer of the arterial wall should be investigated. Instead of only finding the effect of wall shear stress on the LDL concentration at lumen and endothelium interface, our work analyzes the mass transfer in the arterial wall. The concentration profile in the concentration boundary layer of lumen was specified by utilizing information found in the related literature. Our work paves the way for combining the effect of wall shear stress on the LDL concentration at the lumen and endothelium interface and the mechanism of the mass transfer in each layer of the arterial wall.

The main purpose of this work is to investigate the LDL transport within curved arterial layers and investigate the relationship between the LDL concentration at the lumen and endothelium interface and the concentration distribution within the arterial wall. In this work, for the first time in the literature, we have derived the analytical concentration distribution in the curved arterial wall by utilizing the multi-layer arterial model. Though several studies on curved 3D arterial models have been conducted, these works were mainly based on presenting numerical results. Previous analytical works for the curved artery has considered the arterial wall as a simple boundary condition and mainly concentrated on the flow in the lumen. However, the arterial wall structure is complicated and mass transfer inside each layer of the arterial wall must

be accounted for. As such the current work is very important to benefit and improve the prior results.

THEORETICAL MODELING AND ANALYSIS

Wall Model

Earlier research works have also been done related to the arterial model[4,8,26,27] based an imaging approach. Auer *et al.*[5] presented a 3D construction of tissue components in an artery with an atherosclerotic plaque. Cilla *et al.*[9,10] investigated the mathematical modeling of atheroma plaque formation and the role of the morphology on plaque rupture. *In vitro* vascular MR images approach for segmentation of an artery with an atherosclerotic plaque has been presented by Yang *et al.*[29] Malvè *et al.*[18] investigated mass transfer within a rabbit tracheal wall by CT-images, computer simulations and experimental study. Saez *et al.*[22] studied the computational modeling of hypertensive growth in the human carotid artery. MRI and image processing have also been utilized for modeling of an artery Kiousis *et al.*,[14] Auer *et al.*[6]. Liu *et al.*[15–17] constructed the numerical model for 3D curved artery and presented the effect of high pressure and pulsatile blood flow.

Figure 1 shows a typical anatomical structure of an arterial wall[26,27] in this work. It is composed of five layers, i.e., glycocalyx, endothelium, internal elastic lamina, media and adventitia.[4,8] Since its average thickness is only 60 nm, the glycocalyx is generally not considered in the model. Endothelium, a layer of cells interconnected with intercellular junctions is considered followed by IEL, which is composed of an impermeable elastic tissue with fenestral pores. The intima consists of proteoglycan and collagen fibers and the media layer contains smooth muscle cells and elastic connective tissue, comprised of lymphatic and vasa vasorum, which is loosely connected to the adventitia. The thickness and physiological properties of each layer is shown in Table 1.[8,27]

Governing Equations

Figure 1 shows the arterial wall representation with four different macroscopically homogeneous porous layers. The lumen is assumed to be Newtonian and incompressible with constant properties.[1–3,24] The momentum and mass transport equations in the lumen are:

$$\nabla \cdot \mathbf{V} = 0, \tag{1}$$

$$\rho \frac{D\mathbf{V}}{Dt} = -\nabla p + \mu \nabla^2 \mathbf{V}, \tag{2}$$

$$\frac{\partial c}{\partial t} + \mathbf{V} \cdot \nabla c = D\nabla^2 c, \tag{3}$$

where V is the velocity vector, c represents LDL concentration, p represents hydraulic pressure and ρ, μ, and D are the fluid density, viscosity, and diffusivity respectively.

The volume-averaged equations including Forchheimer term are used for transport within the arterial wall. The Staverman filtration coefficient in the concentration equation represents the selective permeation of species by the membrane[13,27,28]

$$\nabla \cdot \mathbf{V} = 0, \tag{4}$$

$$\frac{\mu}{K}\mathbf{V} = -\nabla p - \frac{\rho F \delta}{\sqrt{K}}[\mathbf{V} \cdot \mathbf{V}]J, \tag{5}$$

$$\frac{\partial c}{\partial t} + (1 - \sigma_f)\mathbf{V} \cdot \nabla c = D_e \nabla^2 c + kc, \tag{6}$$

where δ is the porosity; K permeability; σ_f the Staverman filtration coefficient; D_e effective LDL diffusivity, F dimensionless inertia coefficient, J the unit vector oriented along the velocity vector $\mathbf{V}$, k reaction coefficient which is non-zero only inside the media layer and is zero for the other layers.

Boundary Conditions

The velocity profile within the lumen is assumed to be fully developed. At the inlet, the lumen is governed by a fully developed parabolic velocity profile

$$u = u_{max}(1 - (r/r_0)^2), \tag{7}$$

where u_{max} is the centerline velocity, r_0 the radius of the lumen, u the streamwise component of the velocity vector and r is the radial location.

The velocity continuity at the interface between different layers is employed and constant pressure at the outlet of the lumen is applied. The boundary conditions on the concentration equations are:

(1) $c/c_0 = 1$ at the lumen inlet and the LDL concentration at the entrance is taken as $c_0 = 28.6 \times 10^{-3}$ mol/molm^3 m^3[13] based on the typical physiological data.
(2) Concentration at the interface between lumen and endothelium is designated as $c = c_w$.
(3) The species concentration is taken to be zero at the media/adventitia interface.
(4) The continuity of species concentration and the total species flux are incorporated at each interface between the lumen, endothelium, intima, IEL and media. At the interface

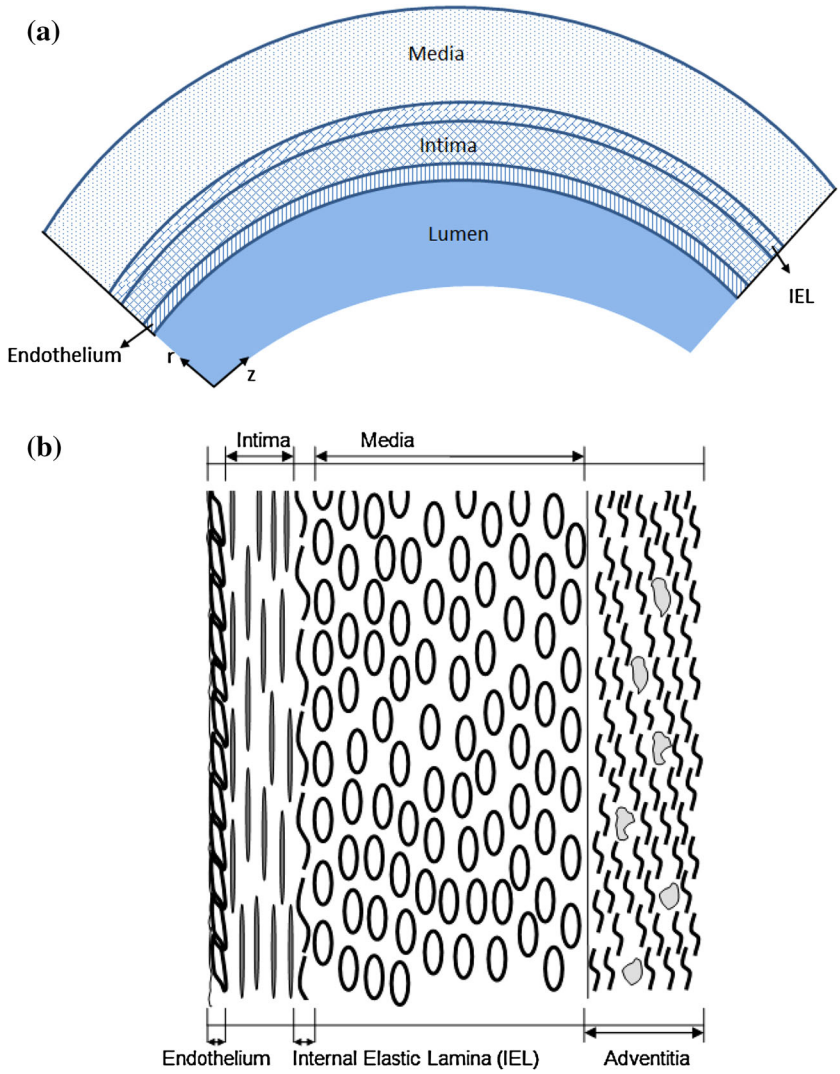

FIGURE 1. (a) Schematic of different arterial layers with curvature (b) partial enlargement view displaying different physical attributes.

TABLE 1. Property values for different arterial layers.

		Lumen	Endothelium	Intima	IEL	Media	Adventitia
Density	ρ (kg/kgmm^3 mm^3)	1070	1057	1057	1057	1057	1057
Diffusivity	D_{eff} (m^2/m^{2}s s)	2.87×10^{-11}	6×10^{-17}	5.4×10^{-12}	3.18×10^{-15}	5×10^{-14}	
Permeability	K (m^2)		4.32×10^{-21}	2×10^{-16}	4.392×10^{-19}	2×10^{-18}	
Porosity	δ		5×10^{-4}	0.983	0.002	0.258	
Reaction coefficient	k (s^{-1})	0	0	0	0	3.197×10^{-4}	
Refection coefficient	σ_{f}		0.9979	0.8272	0.9827	0.8836	
Thickness	H (μm)	3100	2	10	2	200	100
Viscosity	μ_{eff} [kg/(m s)]	3.7×10^{-3}	0.72×10^{-3}	0.72×10^{-3}	0.72×10^{-3}	0.72×10^{-3}	

between lumen and endothelium, the species flux continuity can be expressed as:

$$\left[\mathrm{v}c - D_{\text{e}}\frac{\partial c}{\partial n}\right]|_{-} = \left[(1-\sigma_f)\mathrm{v}c - D_{\text{e}}\frac{\partial c}{\partial n}\right]|_{+}. \quad (8)$$

For other interfaces, the flux continuity can be expressed as:

$$\left[(1-\sigma_{\text{f}})\mathrm{v}c - D_{\text{e}}\frac{\partial c}{\partial n}\right]|_{-} = \left[(1-\sigma_f)\mathrm{v}c - D_{\text{e}}\frac{\partial c}{\partial n}\right]|_{+}. \quad (9)$$

TABLE 2. Streamwise velocity at each arterial layer.

Streamwise velocity	m/s	Artery wall layers
U_1	1.558×10^{-15}	Endothelium
U_2	7.230×10^{-11}	Intima
U_3	1.365×10^{-13}	IEL
U_4	5.564×10^{-14}	Media

METHODOLOGY AND VALIDATION

Fluid Flow Analysis

Darcy-Forchheimer equation is utilized to get the streamwise component of the velocity vector in the arterial wall

$$\frac{\mu}{K}\langle \mathbf{V} \rangle = -\nabla \langle p \rangle - \frac{\rho F \delta}{\sqrt{K}} [\langle \mathbf{V} \rangle \cdot \langle \mathbf{V} \rangle] J. \tag{10}$$

By using the properties in Table 1, the value of the streamwise component of the velocity is solved and presented in Table 2.

Filtration velocity is given in terms of its driving force,

$$u_{\text{filt}} = \frac{p_1 - p_2}{R_{\text{tot}}}, \tag{11}$$

where the total filtration resistance is

$$R_{\text{tot}} = \left(\frac{\mu_{\text{end}} \ln\left(\frac{r_1^o}{r_1^i}\right)}{K_{D_{\text{eff,end}}}} + \frac{\mu_{\text{int}} \ln\left(\frac{r_2^o}{r_2^i}\right)}{K_{D_{\text{eff,int}}}} + \frac{\mu_{\text{iel}} \ln\left(\frac{r_3^o}{r_3^i}\right)}{K_{D_{\text{eff,iel}}}} + \frac{\mu_{\text{med}} \ln\left(\frac{r_4^o}{r_4^i}\right)}{K_{D_{\text{eff,med}}}} \right) r, \tag{12}$$

where r_j^i and r_j^o are the start and the end of the radial coordinate for each arterial wall layer j, respectively.

By using the properties in Table 1 the filtration velocities are calculated to be $\frac{2.294\times10^{-8}}{r^+}$ m/s and $\frac{5.244\times10^{-8}}{r^+}$ m/s for transmural pressure differentials of 70 and 160 mmHg respectively, where r^+ is the non-dimensional radius. This is also reported by Khakpour and Vafai.[13] As can be seen the filtration velocity is much larger than the calculated streamwise velocity given in Table 2. This is due to a much larger transmural pressure as compared to the pressure difference in either axial or circumferential direction. Comparison between the value of filtration velocity and streamwise velocity shows that the filtration velocity is responsible for the primary convective effects. The radial pressure difference is the main force for the fluid flow in the arterial wall and the velocity in axial and circumferential direction can be neglected in the arterial wall. This is also established in Yang and Vafai's work.[27]

Mass Transport

Figure 2 shows the coordinate system of a slightly curved artery. The species concentration equation in the lumen for a curved artery can be written as[23]:

$$v_{\text{r}} \frac{\partial c}{\partial r} + \frac{v_\psi}{r} \frac{\partial c}{\partial \psi} + v_{\text{z}} \frac{R}{R + r \sin\psi} \frac{\partial c}{\partial z} = D_{\text{e}} \frac{1}{r} \frac{\partial}{\partial r} \left(r \frac{\partial c}{\partial r} \right), \tag{13}$$

where R is the radius of the curvature, v_{r} is the velocity in the radial direction, v_{z} is the velocity in the axial direction and v_ψ is the velocity in the circumferential direction.

Our model has been simplified to a two-dimensional one after a comprehensive analysis and full consideration of the three dimensional aspects. The three-dimensional Eq. (13) has been simplified due to a much larger transmural pressure as compared to the pressure difference in either axial or circumferential direction. Comparison between the value of filtration velocity and streamwise velocity shows that the filtration velocity is responsible for the primary convective effects. The radial pressure difference is the main force for the fluid flow in the arterial wall and the velocity in axial and circumferential direction can be neglected in the arterial wall.

Mass Transport Without a Reaction

Due to the physiological properties of the arterial wall, the axial and secondary flow velocities are much smaller than the filtration velocity. Thus the impact of advection caused by v_{z} and v_ψ from Eq. (13) can be neglected. The governing species conservation equation within an arterial wall without a reaction term is then given by

$$(1 - \sigma_{\text{f}}) v_{\text{r}} \frac{\partial c}{\partial r} = D_{\text{e}} \frac{1}{r} \frac{\partial}{\partial r} \left(r \frac{\partial c}{\partial r} \right), \tag{14}$$

where filtration velocity is $v_{\text{f}} = \frac{m}{r^+}$, $m = 2.294 \times 10^{-8}$ m/s for a typical transmural pressure of 70 mmHg and r^+ is the non-dimensional radial coordinate $r^+ = r/r_0$. The non-dimensional form of this equation can be written as

$$B \frac{\partial c}{\partial r^+} = E \frac{\partial}{\partial r^+} \left(r^+ \frac{\partial c}{\partial r^+} \right), \tag{15}$$

where $B = (1-\sigma_{\text{f}})m/r_0$, $E = D_{\text{e}}/r_0^2$, and r_0 is the radius of the artery (the lumen part).

This equation can be applied to endothelium, intima, IEL and media. The general form of the solution for this equation is:

$$c(r) = C_1^i \times \frac{E_i r^{+\frac{B_i}{E_i}}}{B_i} + C_2^i, \tag{16}$$

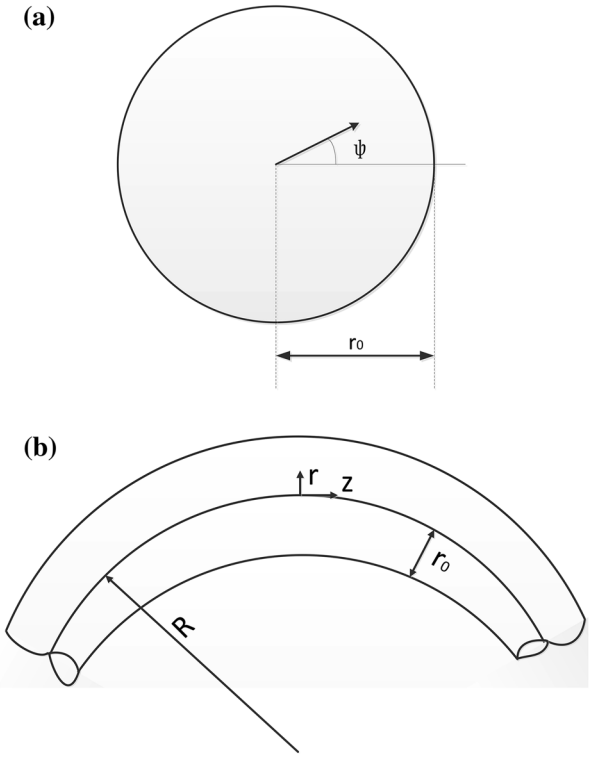

FIGURE 2. Coordinate system for a curved artery.

where C_1^i and C_2^i are the unknown coefficients for the arterial wall layer i ($i = 1, 2, 3$ for lumen, intima and IEL respectively). As discussed later, the values of these coefficients are given in Table 3.

Mass Transport in the Presence of a Reaction

The chemical reaction should be considered for the mass transport within the media layer, which is modeled as an irreversible first-order reaction. The non-dimensional species concentration equation for the media layer can be written as

$$\frac{B_4}{r^+}\frac{\partial c}{\partial r^+} = E_4\frac{1}{r^+}\frac{\partial}{\partial r^+}\left(r^+\frac{\partial c}{\partial r^+}\right) - kc, \tag{17}$$

where k is the chemical reaction rate.

The solution for this equation is found to be:

$$c(r) = C_1^4 \times r^{+\frac{B}{2E}} I_{\frac{B}{2E}}\left(\frac{\sqrt{k}}{\sqrt{E}}r^+\right) + C_2^4 \times r^{+\frac{B}{2E}} K_{\frac{B}{2E}}\left(\frac{\sqrt{k}}{\sqrt{E}}r^+\right), \tag{18}$$

where $I_{\frac{B}{2E}}(\frac{\sqrt{k}}{\sqrt{E}}r^+)$ is the modified Bessel functions of 1st kind and $K_{\frac{B}{2E}}(\frac{\sqrt{k}}{\sqrt{E}}r^+)$ is Modified Bessel functions of 2nd kind. C_1^4 and C_2^4 are the unknown coefficients for the media layer.

In the expression for the concentration distribution within the arterial wall, 8 unknown parameters exist. These are C_1^i and C_2^i ($i = 1, 2, 3, 4$ for lumen, intima, IEL and media respectively). As such, eight boundary conditions are utilized to solve these unknowns. These are

at lumen/endothelium interface:

$$c(r)|_+ = c_w. \tag{19}$$

at endothelium/intima, intima/IEL, IEL/media interfaces:

$$c(r)|_+ = c(r)|_-, \tag{20}$$

$$\left[\mathrm{Bc} - \mathrm{Er}\frac{\partial c}{\partial r}\right]|_- = \left[\mathrm{Bc} - \mathrm{Er}\frac{\partial c}{\partial r}\right]|_+. \tag{21}$$

and lastly at the media/adventitia interface:

$$\frac{\partial c}{\partial n}|_- = 0 \tag{22}$$

Physiological property values in Table 1 are utilized to solve for C_1^i and C_2^i. Table 3 presents the solutions for C_1^i and C_2^i, which are given in terms of the lumen/endothelium interface concentration c_w.

Validation

In an artery without a curvature, secondary flow does not exist in the lumen. In order to compare the analytical solution with prior works, we assume the non-dimensional concentration at the lumen/endothelium interface can be presented by $c_w = 1$. By utilizing the calculated coefficients given in Table 3, the concentration distributions in each of the arterial wall layers can be derived. Figures 3 and 4 show the comparison between the current analytical results for the concentration distribution in different layers of a straight arterial wall with either Yang and Vafai[27] or Stephen and Vafai[8] using the physiological properties given in each of these works respectively.

For the validation, we are comparing the results that we have derived for a curved artery in the limit when the radius of curvature is large with the results for a straight artery. The radial pressure difference is the main force for the fluid flow in the arterial wall and the velocity in axial and circumferential direction can be neglected in the arterial wall. Thus the LDL concentration at lumen and endothelium interface will be the critical aspect for the concentration distribution in the arterial wall. If we utilize the $c_w = 1$ at the lumen/endothelium interface, then the result should agree with the previous results for a straight artery. Though the governing equations are expressed in different coordinate systems, the results agree quite well with each other. The reason for this agreement is that the radius of lumen is much larger than the thickness of arterial wall layers. Thus on a local basis, it is

TABLE 3. Values of coefficients C_1^i and C_2^i: Based on utilizing properties in Yang and Vafai's work[27] under 70 mmHg and 160 mmHg transmural pressure and Based on utilizing physiology properties in Stephen and Vafai's work[8] under 70 mmHg transmural pressure.

(a)

	70 mmHg		160 mmHg	
Artery wall layers	C_1^i	C_2^i	C_1^i	C_2^i
Endothelium	$-602.548\ c_w$	$1.243\ c_w$	$-139.728\ c_w$	$1.025\ c_w$
Intima	$0.0598\ c_w$	$0.0150\ c_w$	$0.2513\ c_w$	$0.0124\ c_w$
IEL	$-9.432\ c_w$	$0.150\ c_w$	$-1.814\ c_w$	$0.124\ c_w$
Media	$2.492 \times 10^{-118}\ c_w$	$1.574 \times 10^{101}\ c_w$	$2.419 \times 10^{-97}\ c_w$	$1.351 \times 10^{77}\ c_w$

(b)

Artery wall layers	C_1^i	C_2^i
Endothelium	$-0.396 \times 10^{-33}\ c_w$	c_w
Intima	$0.231\ c_w$	$0.0584\ c_w$
IEL	$-36.658\ c_w$	$0.583\ c_w$
Media	$9.687 \times 10^{-118}\ c_w$	$6.117 \times 10^{101}\ c_w$

reasonable to assume the surface is flat. The agreement between the analytical results which account for the curvature effect and the numerical results which are based on a flat layout of the arterial layers verifies the correct representations of the cited prior works.

Figure 5 displays LDL concentration within different layers under 70 and 160 mmHg transmural pressure across the arterial wall. The agreement in the results establishes that the pertinent physical attributes are properly incorporated within our analytical solution. The figures also show that neglecting the streamwise velocity doesn't affect the result.

EFFECT OF THE CURVATURE

For a curved artery, secondary flow exists in the lumen region. The velocity region can be divided into two regions, a core region and the boundary layer respectively.[30] In the same way, the concentration in the lumen can also be divided into two regions, concentration core region and the boundary layer region, as shown in Fig. 6. The concentration distribution in the concentration core region is considered to be uniform and it is not affected by the boundary.

The non-dimensional concentration boundary layer thickness is defined as $\Delta^+ = \Delta/r_0$, where r_0 is the radius of the artery. Thus the concentration boundary layer region is from $r^+ = 1 - \Delta^+$ to $r^+ = 1$.[23] Introducing $y^+ = 1 - r^+$, then the region is from $y^+ = \Delta^+$ to $y^+ = 0$. According to Srinivasan and Chi's work,[23] concentration profile in the boundary layer can be assumed as:

$$c = a_1 + a_2\frac{y^+}{\Delta^+} + a_3\left(\frac{y^+}{\Delta^+}\right)^2, \tag{23}$$

where a_1, a_2, a_3 are the coefficients which can be determined by the boundary conditions imposed on the concentration boundary layer. This concentration profile utilizes the average concentration in the circumferential direction. The boundary conditions are listed as follows:

At the interface of the concentration core region and the boundary layer ($y^+ = \Delta^+$):

$$c = 1, \quad \frac{\partial c}{\partial y^+} = 0 \tag{24}$$

At the interface of lumen and endothelium ($y^+ = 0$):

$$c(y=0)|_{\text{Lumen}} = c(y=0)|_{\text{endothelium}},$$

$$\left[vc - D_e\frac{\partial c}{\partial n}\right]|_{\text{Lumen}} = \left[(1-\sigma_f)vc - D_e\frac{\partial c}{\partial n}\right]|_{\text{endothelium}}. \tag{25}$$

Also for small axial coordinate z^+, the thickness of the concentration boundary layer can be expressed as[23]:

$$\Delta^+ = \left[\frac{24}{(L_1)(N_{Sc})}\right]^{1/3} z^{+1/3}, \tag{26}$$

where

$$L_1 = \frac{2V^+_{\theta,\delta^+}}{\delta^+}, \tag{27}$$

$$V^+_{\theta,\delta^+} = \frac{1}{1 - \frac{2}{3}\delta^+ + \frac{\delta^{+2}}{6}}, \tag{28}$$

$$\delta^+ = \frac{4.6311}{\mathrm{Dn}^{1/2}} - \frac{0.7659}{\mathrm{Dn}}, \tag{29}$$

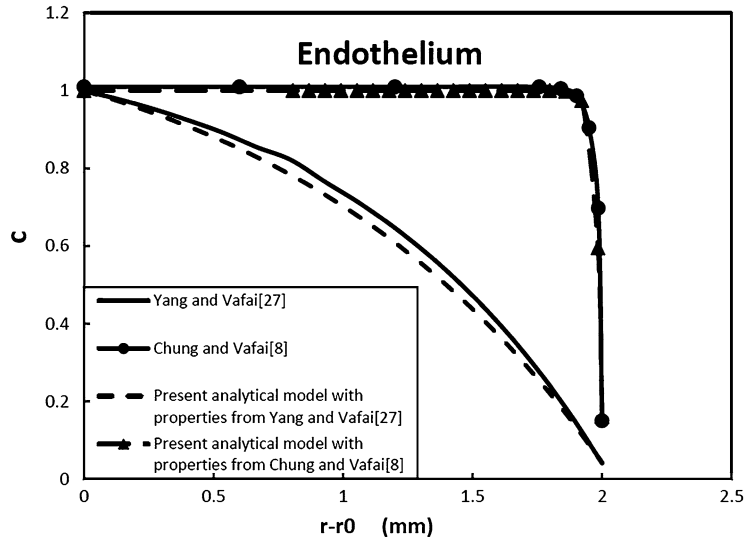

(a) Endothelium

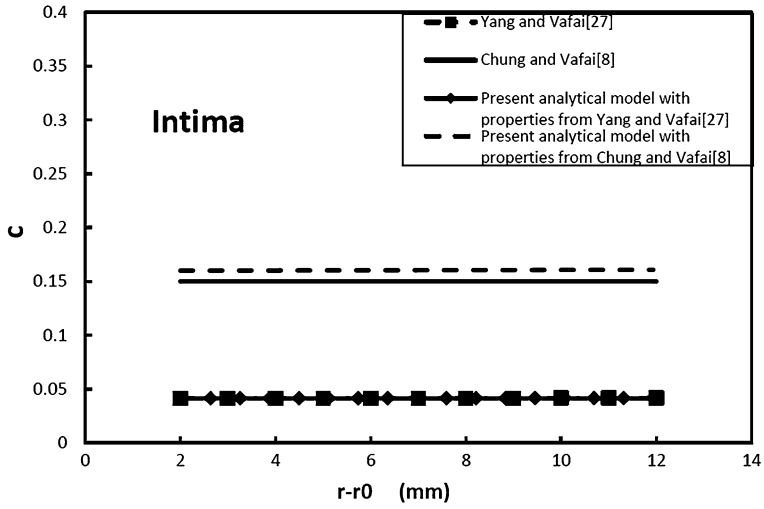

(b) Intima

FIGURE 3. Comparison of our analytical results with prior numerical results for the LDL concentration distributions across (a) Endothelium, (b) Intima under 70 mmHg transmural pressure difference across the artery wall.

$$\mathrm{Dn} = 2\lambda^{\frac{1}{2}}\mathrm{Re}, \tag{30}$$

$$\lambda = r_0/R \tag{31}$$

$$N_{\mathrm{Sc}} = \frac{v}{\mathrm{De}}, \tag{32}$$

$$z^{+} = \frac{z}{r_0 \mathrm{Re}}. \tag{33}$$

The concentration distribution in the endothelium layer was derived in Eq. (16). The four unknowns a_1, a_2, a_3 and c_w can be obtained by applying the cited four boundary conditions.

RESULTS AND DISCUSSION

Utilizing the physiological properties given in Table 1, and using a radius ratio of $\lambda = 0.1$ and a Reynolds Number Re = 245, which represent typical physiology conditions based on typical values found in the literature for an artery, where mean velocity $U_0 = 16.9$ cm/s is specified.,[23,27] the expression for c_w can be derived as:

$$c_w = \frac{1}{1 - 0.0344 z^{+1/3}}. \tag{34}$$

Figure 7 displays a comparison for concentration distribution at the lumen/endothelium interface

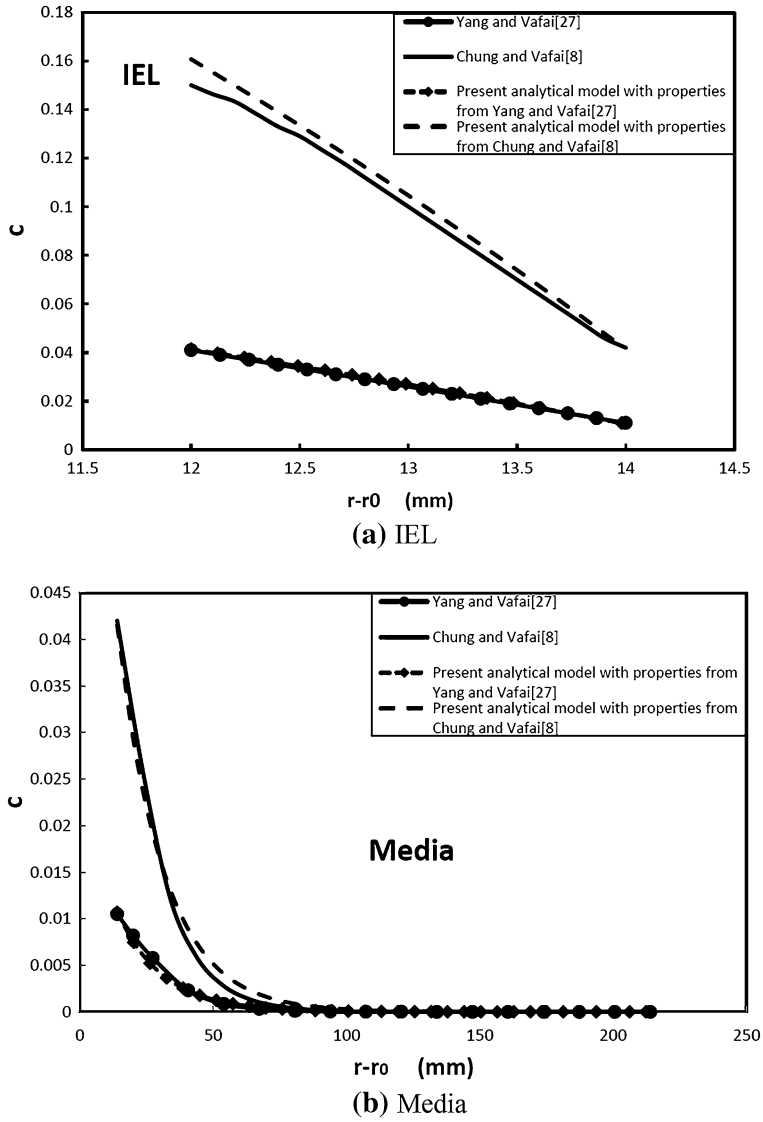

FIGURE 4. Comparison of our analytical results with prior numerical results for the LDL concentration distributions across (a) IEL, (b) Media under 70 mmHg transmural pressure difference across the artery wall.

between a straight (Yang and Vafai[27]) and a curved artery (current analytical work). As can be seen, the concentration at lumen and endothelium interface for the curved artery is smaller than the concentration in the straight artery which agrees with Srinivasan and Chi's work.[23] This reduction is due to the secondary flow formation in the curved artery. The secondary flow or flow separation changes the wall shear stress distribution and inhibits the LDL accumulation within the arterial wall.

Figure 8 displays the curvature effect. As can be seen, decreasing the radius ratio λ results in an increase in the concentration at the lumen/endothelium interface. Effectively, decreasing the radius ratio translates into a larger radius of curvature, thus approaching the straight artery configuration.

Figure 9 illustrates the effects of different Reynolds number on the LDL concentration distribution at the lumen/endothelium interface. As it can be seen, Reynolds number has an impact on the species accumulation at the lumen/endothelium interface. As the Reynolds number increases, the concentration is found to decrease. This can be explained by the increased interaction between fluid and the arterial wall which hinders the LDL accumulation at the interface.

Concentration profiles at different arterial wall layer interfaces are presented in Fig. 10. It can be seen that the concentration changes at lumen and endothelium

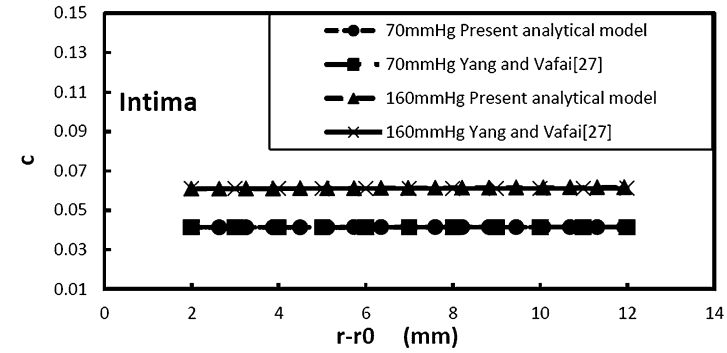

(a) Intima

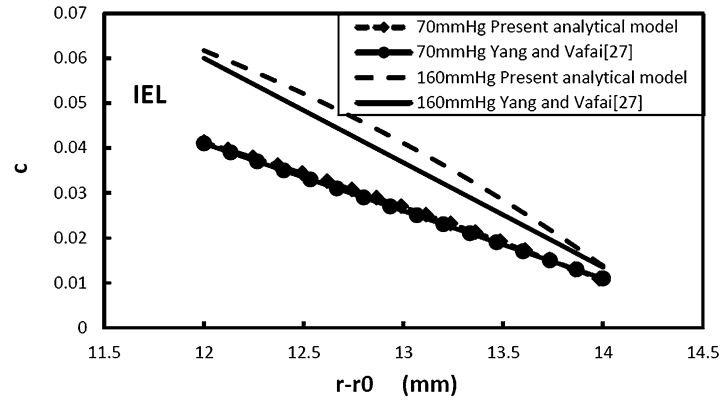

(b) IEL

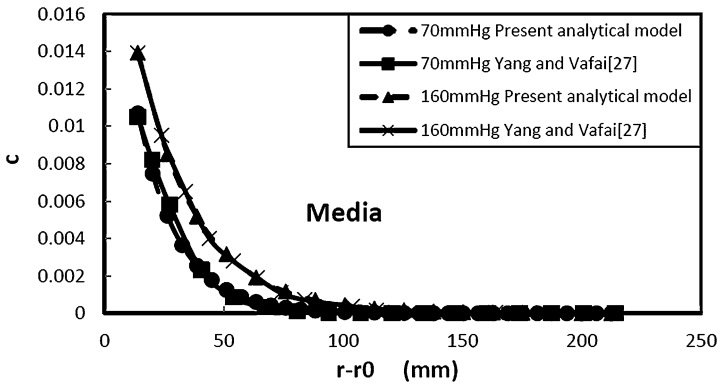

(c) Media

FIGURE 5. Comparison of our analytical results with prior numerical results for the LDL concentration distributions across (a) Intima, (b) IEL, (c) Media under 70 and 160 mmHg transmural pressure difference.

interface in the axial direction plays a minor role in the concentration profiles at other wall layer interfaces.

We fully consider the boundary conditions at the lumen and endothelium interface by first deriving the concentration distribution in the endothelium layer while incorporating the boundary conditions to solve the interface concentration. The derived concentration distribution c_w at the lumen/endothelium interface is utilized to obtain the concentration distributions within the arterial wall. Our results provide a complete analytical description of the LDL concentration distribution within an arterial wall.

CONCLUSIONS

LDL transport in each layer of the curved arterial wall is studied analytically in order to elucidate the mechanisms of atherogenesis and development of anastomotic intimal hyperplasia. The comprehensive

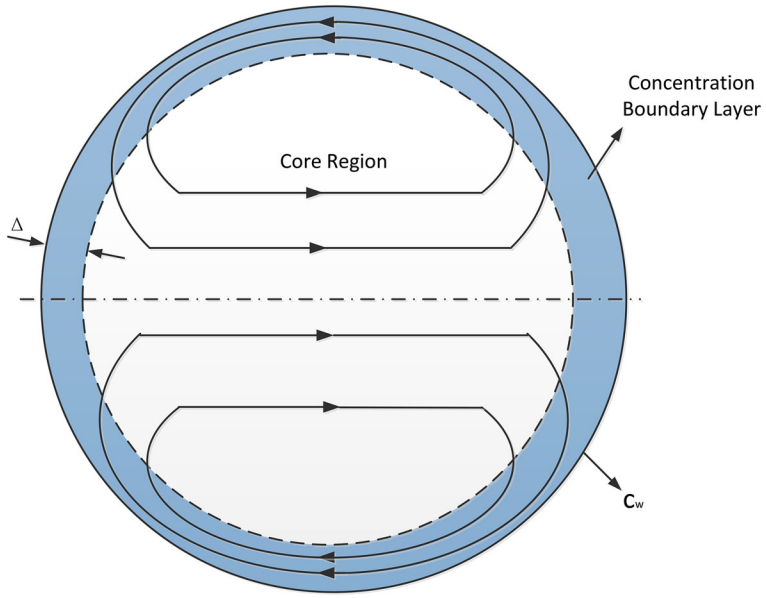

FIGURE 6. Schematic illustration of the concentration boundary layer.

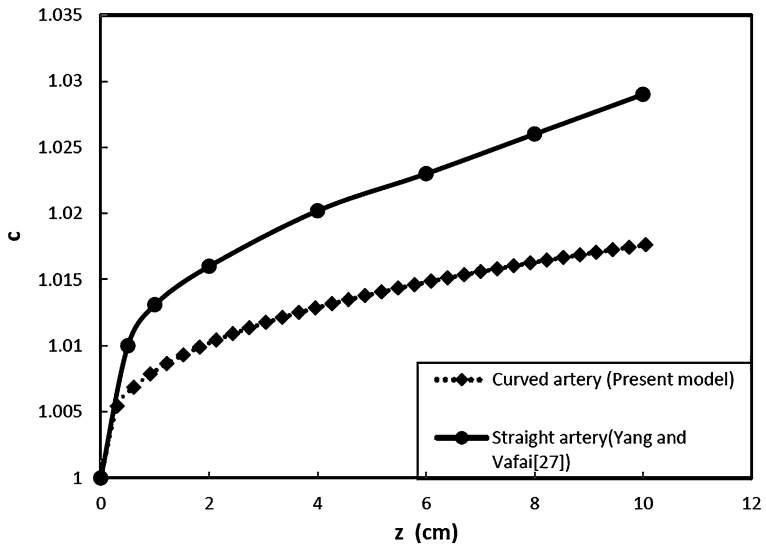

FIGURE 7. Comparison of the concentration distribution along the lumen and endothelium interface between a straight and a curved artery in the axial direction with a radius ratio $\lambda = 0.1$.

concentration distribution expression of LDL in each layer of the curved arterial wall is presented.

Our work aims to analyze the mass transfer in each layer of the curved artery wall and how the concentration polarization at lumen and endothelium interface affects the concentration distribution in the arterial wall. A concentration profile in the boundary layer of the lumen was incorporated based on prior research works. We have solved and analyzed the concentration distribution at the lumen and endothelium interface, which contains the information related to the concentration polarization. This concentration distribution is the average value in the circumferential direction.

The concentration inside the arterial wall layers incorporates the concentration at the interface of lumen and endothelium, which is affected by the secondary and recirculation flows. The result shows that the average concentration in the axial direction is actually decreasing in the curved artery compared

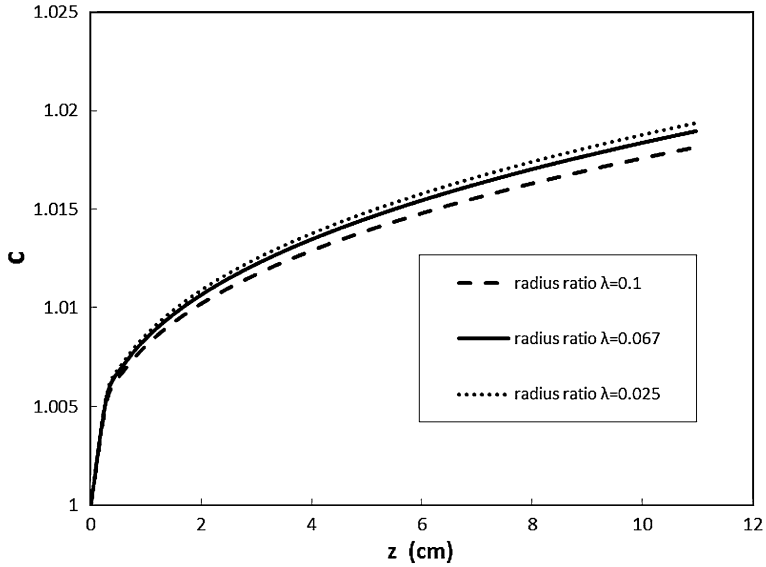

FIGURE 8. Effect of the curvature on LDL concentration at the lumen/endothelium interface along the axial direction.

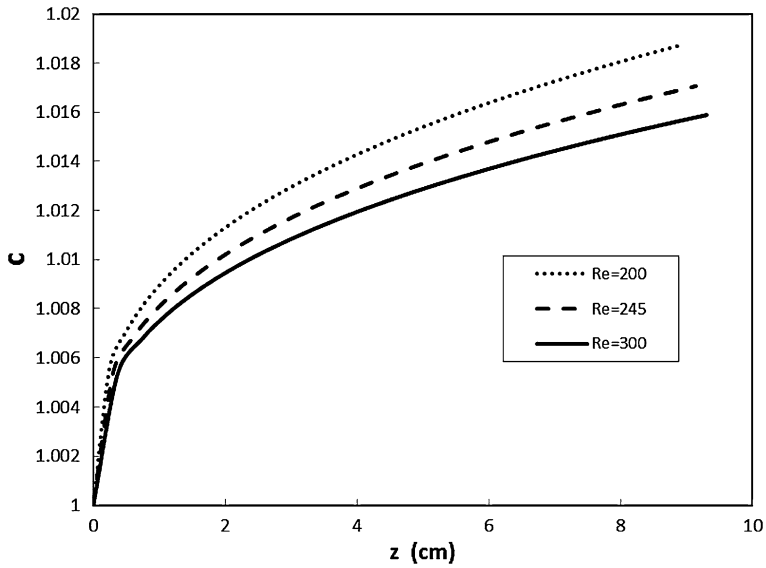

FIGURE 9. Effect of the Reynolds Number on the concentration distributions along the lumen/endothelium interface in the axial direction.

with straight artery. Based on our analytical results we have also established that small radius ratio and Reynolds number will augment the LDL accumulation at lumen endothelium interface. Furthermore, we have shown that an increase in the LDL concentration at the lumen/endothelium interface in the axial direction has a minor effect on the concentration profile at other wall layer interfaces. Thus the preferential localization of atherosclerotic disease in the curved artery is caused by the concentration polarization in the circumferential direction. Secondary and recirculation flows cause the uneven shear stress distribution in the circumferential direction. The shear stress causes the concentration polarization at the interface of lumen and endothelium and finally causes the concentration changes in the arterial wall. More studies are needed to establish the effect of shear stress distribution on the concentration polarization at the interface of lumen/endothelium in the circumferential direction and to achieve more accurate concentration distribution at the lumen/endothelium interface.

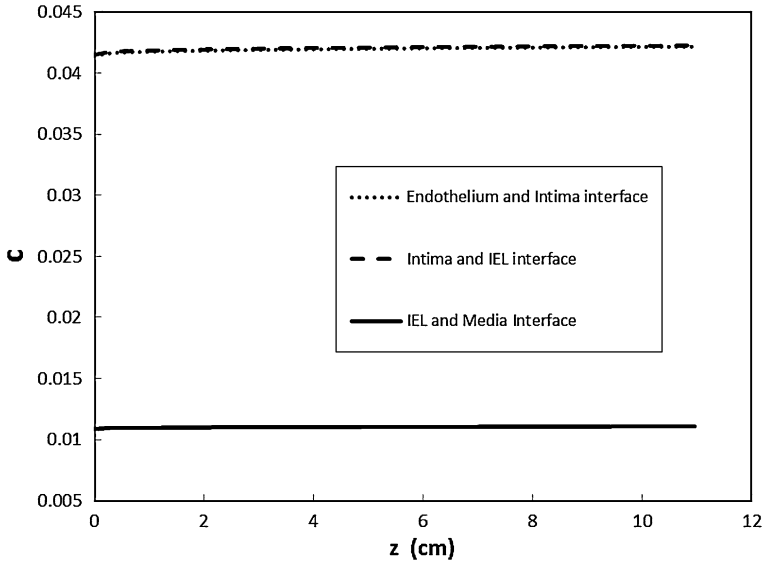

FIGURE 10. Concentration distributions along the axial direction at different arterial wall layer interfaces.

CONFLICT OF INTEREST

There is no conflict of interest. This manuscript has not been submitted to anywhere else.

REFERENCES

[1]Abraham, J. P., E. M. Sparrow, and R. D. Lovik. Unsteady, three-dimensional fluid mechanic analysis of blood flow in plaque-narrowed and plaque-free arteries. *Int. J. Heat Mass Transf.* 51:5633–5641, 2008.

[2]Abraham, J. P., E. M. Sparrow, J. M. Gorman, J. R. Stark, and R. E. Kohler. A mass transfer model of temporal drug deposition in artery walls. *Int. J. Heat Mass Transf.* 58:632–638, 2013.

[3]Abraham, J. P., J. R. Stark, J. M. Gorman, E. M. Sparrow, and R. Kohler, A model of drug deposition within artery walls. *J. Med. Dev.* 7, Paper No. 020902, 2013.

[4]Ai, L., and K. Vafai. A coupling model for macromolecule transport in a stenosed arterial wall. *Int. J. Heat Mass Transf.* 49:1568–1591, 2006.

[5]Auer, M., R. Stollberger, P. Regitnig, F. Ebner, and G. A. Holzapfel. 3-D reconstruction of tissue components for atherosclerotic human arteries using ex vivo high-resolution MRI. *IEEE T. Med. Imaging* 25:345–357, 2006.

[6]Auer, M., R. Stollberger, P. Regitnig, F. Ebner, and G. A. Holzapfel. In vitro angioplasty of atherosclerotic human femoral arteries: analysis of the geometrical changes in the individual tissues using MRI and image processing. *Ann. Biomed. Eng.* 38:1276–1287, 2010.

[7]Chang, L., and J. M. Tarbell. Numerical simulation of fully developed sinusoidal and pulsatile (physiological) flow in curved tubes. *J. Fluid Mech.* 161:175–198, 1985.

[8]Chung, S., and K. Vafai. Low-density lipoprotein transport within a multi-layered arterial wall-effect of the atherosclerotic plaque/stenosis. *J. Biomech.* 46:574–585, 2013.

[9]Cilla, M., E. Peña, and M. A. Martinez. 3D computational parametric analysis of eccentric atheroma plaque: influence of axial and circumferential residual stresses. *Biomech. Model. Mechanobiol.* 11:1001–1013, 2012.

[10]Cilla, M., E. Peña, and M. A. Martinez. Mathematical modelling of atheroma plaque formation and development in coronary arteries. *J. R. Soc. Interface* 11:20130866, 2014.

[11]Dash, R. K., G. Jayaraman, and K. N. Mehta. Flow in a catheterised curved artery with stenosis. *J. Biomech.* 32:49–61, 1999.

[12]Dennis, S. C. R., and M. Ng. Dual solutions for steady laminar flow through a curved tube. *Q. J. Mech. Appl. Math.* 35:305–324, 1982.

[13]Khakpour, M., and K. Vafai. A comprehensive analytical solution of macromolecular transport within an artery. *Int. J. Heat Mass Transf.* 51:2905–2913, 2008.

[14]Kiousis, D. E., T. C. Gasser, and G. A. Holzapfel. A numerical model to study the interaction of vascular stents with human atherosclerotic lesions. *Ann. Biomed. Eng.* 35:1857–1869, 2007.

[15]Liu, X., F. Pu, Y. Fan, X. Deng, D. Li, and S. Li. A Numerical study on the flow of blood and the transport of LDL in the human aorta: the physiological significance of the helical flow in the aortic arch. *Am. J. Physiol. Heart Circ. Physiol.* 297(1):H163–H170, 2009.

[16]Liu, Xiao, Yubo Fan, and Xiaoyan Deng. Effect of the endothelial glycocalyx layer on arterial LDL transport under normal and high pressure. *J. Theor. Biol.* 283(1):71–81, 2011.

[17]Liu, X., Y. Fan, X. Deng, and F. Zhan. Effect of non-newtonian and pulsatile blood flow on mass transport in the human aorta. *J. Biomech.* 44(6):1123–1131, 2011.

[18]Malvè, M., C. Serrano, E. Peña, R. Fernández-Parra, F. Lostalé, M. A. De Gregorio, and M. A. Martinez. Modelling the air mass transfer in a healthy and a stented rabbit trachea: CT-images, computer simulations and experimental study. *Int. Commun. Heat. Mass* 53:1–8, 2014.

[19]Padmanabhan, N., and G. Jayaraman. Flow in a curved tube with constriction—an application to the arterial system. *Med. Biol. Eng. Comput.* 22:216–224, 1984.

[20]Qiao, A. K., X. L. Guo, S. G. Wu, Y. J. Zeng, and X. H. Xu. Numerical study of nonlinear pulsatile flow in S-shaped curved arteries. *Med. Eng. Phys.* 26:545–552, 2004.

[21]Rosamond, W., K. Flegal, G. Friday, *et al*. Heart disease and stroke statistics—2007 update: a report from the American Heart Association Statistics Committee and Stroke Statistics Subcommittee. *Circulation* 115:69–171, 2007.
[22]Sáez, P., E. Peña, M. A. Martínez, and E. Kuhl. Computational modeling of hypertensive growth in the human carotid artery. *Comput. Mech*. 53:1183–1196, 2014.
[23]Srinivasan, S., and T. Chi. Reverse osmosis in a curved tubular membrane duct. *Desalination* 9(2):127–139, 1971.
[24]Stark, J. R. J. M., E. M. Gorman, J. P. Sparrow, and R. E. Abraham. Kohler. Controlling the rate of penetration of a therapeutic drug into the wall of an artery by means of a pressurized balloon. *J. Biomed. Sci. Eng*. 6:527–532, 2013.
[25]Wada, S., and T. Karino. Theoretical prediction of low-density lipoproteins concentration at the luminal surface of an artery with a multiple bend. *Ann. Biom. Eng*. 30:778–791, 2002.
[26]Wang, S., and K. Vafai. Analysis of the effect of stent emplacement on LDL transport within an artery. *Int. J. Heat Mass Transf*. 64:1031–1140, 2013.
[27]Yang, N., and K. Vafai. Modeling of low-density lipoprotein (LDL) transport in the artery—effects of hypertension. *J. Int. Heat Mass Transf*. 49:850–867, 2006.
[28]Yang, K., and K. Vafai. Analysis of heat flux bifurcation inside porous media incorporating inertial and dispersion effects-an exact solution. *Int. J. Heat Mass Transf*. 54:5286–5297, 2011.
[29]Yang, F., G. Holzapfel, C. Schulze-Bauer, R. Stollberger, D. Thedens, L. Bolinger, A. Stolpen, and M. Sonka. Segmentation of wall and plaque in in vitro vascular MR images. *Int. J. Cardiovasc. Imaging* 19:419–428, 2003.
[30]Yasuo, M., and N. Wataru. Study on forced convective heat transfer in curved pipes: (1st report, laminar region). *Int. J. Heat Mass Transf*. 8(1):67–82, 1965.